2020

Epstein Barr virus-immortalized B lymphocytes exacerbate experimental autoimmune encephalomyelitis in xenograft mice

Pascal Polepole
University of Nebraska - Lincoln

Alison Bartenslager
University of Nebraska - Lincoln, alison.bartenslager@huskers.unl.edu

Yutong Liu
University of Nebraska Medical Center, yutongliu@unmc.edu

Thomas M. Petro
University of Nebraska-Lincoln, tpetro@unmc.edu

Samodha C. Fernando
University of Nebraska - Lincoln, samodha@unl.edu

See next page for additional authors

Luwen Zhang ORCID iD: 0000-0002-1621-8034

Epstein Barr virus-immortalized B lymphocytes exacerbate experimental autoimmune encephalomyelitis in xenograft mice

Pascal Polepole[1], Alison Bartenslager[2], Yutong Liu[4], Thomas M. Petro[5], Samodha Fernando[2], and Luwen Zhang[1,3]*

Nebraska Center for Virology[1],

Department of Animal Science[2], School of Biological Sciences[3], University of Nebraska, Lincoln, NE 68583. Department of Radiology[4], Dept. of Oral Biology[5], University of Nebraska Medical Center, Omaha, NE 68198

Running head: EBV and MS connections

* Corresponding author:

Luwen Zhang,

Professor of Biological Sciences

Nebraska Center for Virology

University of Nebraska

238 Morrison Center

4240 Fair Street

Lincoln, NE 68583-0900

Tel: 402-472-5905

Fax: 402-472-3323

Email: lzhang2@unl.edu

This article has been accepted for publication and undergone full peer review but has not been through the copyediting, typesetting, pagination and proofreading process, which may lead to differences between this version and the Version of Record. Please cite this article as doi: 10.1002/jmv.26188.

Abstract

Multiple sclerosis (MS) is the most common autoimmune disorder affecting the central nervous system. Epstein-Barr virus (EBV) is a causative agent for infectious mononucleosis (IM) that is associated with MS pathogenesis. However, the exact mechanism by which EBV, specifically in IM, increases the risk for MS remains unknown. EBV immortalizes primary B lymphocytes *in vitro* and causes excessive B lymphocyte proliferation in IM *in vivo*. In asymptomatic carriers, EBV-infected B lymphocytes still proliferate to certain degrees, the process of which is tightly controlled by the host immune systems. Experimental autoimmune encephalomyelitis (EAE) mimics key features of MS in humans and is a well-established rodent model for human MS. We have found that xenografts of EBV-immortalized B lymphocytes, which partially resemble the hyperproliferation of EBV-infected cells in IM, exacerbate autoimmune responses in myelin oligodendrocyte glycoprotein-induced EAE in C57BL/6 mice. After remission, an additional challenge with EBV-immortalized cells induces a relapse in EAE. Moreover, xenografts with EBV-immortalized cells tighten the integrity of blood brain barrier (BBB) in thalamus and hypothalamus areas of the mouse brains. Genomic sequences of prokaryotic 16S rRNA presented in feces reveal that EBV-immortalized cells significantly change the diversities of microbial populations. Our data collectively suggest that EBV-mediated proliferation of B lymphocytes may be a risk factor for the exacerbation of MS, which are associated with gut microbiome changes and BBB modulations. Furthermore, multiple xenografts of EBV-immortalized cells into in C57BL/6 mice could sever as a useful model for human relapsing-remitting MS with predictable severity and timing.

Highlights

- Mimic IM with EBV-immortalized cells enhances EAE in C57BL/6 mice
- Changes in BBB and microbiome are associated with the enhancement
- Multiple exposure of EBV-immortalized cells could sever as a model for human relapsing-remitting MS with predictable severity and timing

Key words: Epstein Barr virus, multiple sclerosis, experimental autoimmune encephalomyelitis, gut microbiome, magnetic resonance imaging

1. Introduction

Multiple sclerosis (MS) is the most common autoimmune disorder affecting the central nervous system. Pathogenically, the insulating myelinations of nerve cells in the brain and spinal cord are damaged. Damaged myelin disrupts neuronal communication, resulting in a range of signs and symptoms, including physical, mental, and sometimes psychiatric problems [1]. Although the clinical presentation and course of the disease are highly variable, several MS types are recognized, including relapsing-remitting MS (RRMS) and secondary progressive MS (SPMS) [2,3]. Despite decades of research, the causes of MS, are not yet well understood.

Epstein–Barr virus (EBV) is a member of human herpesvirus family that is associated with several human cancers [4,5]. EBV mainly targets B lymphocytes and epithelial cells. EBV has two major infection stages: lytic and latent infections. The lytic replication cycle results in the production of infectious virions. In latency, only a portion of EBV's genes are expressed. *In vitro*, EBV infects and immortalizes B lymphocytes efficiently and generate continuously growing lymphoblastoid cell lines (LCL) and establish a type III latency [4,6]. In most cases EBV infection is asymptomatic

but some individuals develop self-limiting infectious mononucleosis (IM), whose symptoms are initiated by overproliferation of EBV-infected B lymphocytes, majority of which are type III latency [4,6-9].

Several lines of evidence strongly support the notion that EBV infection is a risk factor for MS pathogenesis: MS patients have universal EBV seropositivity, higher EBV antibody levels in the blood and higher concentrations of virions in the saliva [10-12]. Moreover, MS patients tend to have reduced EBV-specific $CD8^+$ T-cell immunity, but increased EBV-positive B lymphocytes and plasma cells in the brains. Furthermore, spontaneous EBV-induced immortalization of peripheral blood B lymphocytes from MS patients are increased [13-15].

While the association between MS and EBV, particular in IM, is fairly strong, the exact mechanism by which EBV increases the risk of MS remains unknown. Unfortunately, EBV does not infect rodent cells and there is no murine EBV equivalent discovered yet. Therefore, there is a need for generating a rodent MS model incorporating EBV.

Experimental autoimmune encephalomyelitis (EAE) is a well-characterized animal model to study the etiology and pathogenesis of MS [16,17]. By mimicking hyperproliferation of B-lymphocytes in IM *in vivo*, we have discovered that xenografts of EBV-immortalized B lymphocytes exacerbate autoimmune responses in a rodent EAE model. Also, the phenotype of EAE is associated with significant gut microbiota changes and tightening of blood brain barrier (BBB) in certain areas of the mouse brains. The results suggest that overproliferation of EBV-infected B lymphocytes may

be a factor for MS development. Moreover, a novel model for RRMS with predictable severity may be generated.

2. Methods

2.1. Active Induction of EAE and Cell lines

C57BL/6J and APP-null (*app*−/−; B6.129S7-Apptm1Dbo/J) mice were purchased from Jackson Laboratories. All mice were bred and housed at the American Association for Accreditation of Laboratory Animal Care-accredited facility under specific-pathogen-free conditions. C57BL/6 mice are a common strain for modelling EAE, while the amyloid precursor protein (APP)-null strain was derived from C57BL/6 but is more sensitive for EAE induction [18]. All experimental protocols were approved by the Institutional Animal Care and Use Committee (IACUC) and Institutional Biosafety Committee (IBC) of the University of Nebraska–Lincoln and followed federal guideline. All research staffs were trained in animal care or handling. Cells were washed with PBS and desired numbers in PBS were injected into mice in an intraperitoneal (i.p.) manner. Myelin oligodendrocyte glycoprotein peptide (MOG_{35-55}) were synthesized from Novopep Inc in large quantities. An emulsion containing 100 μg of MOG peptide in complete Freund's adjuvant (CFA; *Mycobacterium tuberculosis H37Ra*, 4 mg/mL) was injected subcutaneously on either hind flank as two injections. In addition, 200 ng of pertussis toxin was injected intraperitoneally (ip) on the same day as MOG-CFA, and another dose was administered after 48 h following standard protocol [19]. Clinical EAE symptoms in mice were evaluated daily with: 0.5=partially limp tail,1=paralyzed tail, 2=paralyzed tail and hind limb paresis, 2.5=paralyzed tail and one hind limb, 3=both hind limbs paralyzed, 3.5=both hind limbs paralyzed, fore limbs partially paralyzed,

4=complete hind and fore limb paralysis, 5=moribund [20]. The severity of EAE was scored on daily basis by two researchers, and occasionally a third researcher was used for calibrations. All animal welfare considerations were taken, including efforts to minimize suffering and distress. When a weight loss of 10-15% within a few days or EAE scores 4 or above, those mice were euthanized immediately. The whole experiments took 2-3 months to finish.

EBV-immortalized B lymphocytes from a SPMS patient (MS-LCL) were obtained from Multiple Sclerosis Genetic Susceptibility Project at University of California, San Francisco (UCSF). The immortalized cells were amplified and passaged in tissue culture system constantly and exhibited EBV type III latency based on EBV gene expression and morphology (data not sown). MS-Human EBV-positive Sav I and Sav III cell lines were gifts from Dr. Jeff Sample. The two lines are isogenic with different EBV-latencies (Sav I: type I latency; and SavIII, type III latency). The cells were grown and maintained in Roswell Park Memorial Institute (RPMI) 1640 medium (GIBCO Cat#: 11875135) containing 10% fetal bovine serum (FBS) (Atlanta Biologicals, cat#: S11150) and 1X penicillin-streptomycin (PS) (Thermo Fisher Scientific Cat#: 15140163) in a humidified chamber with 5% CO_2 at 37°C.

2.2. Western Blot Analysis with Enhanced Chemiluminescence (ECL)

Cells were collected and dissolved in 2x SDS loading buffer. Separation of proteins on SDS-PAGE was carried out following the standard protocol. After the proteins were transferred to a nitrocellulose (BIO-RAD, Cat# 1620112), or immobilon membrane (Millipore, IPVH00010), the membranes were placed with Ponceau S stain solution (0.5% Ponceau S in 1% acetic acid) for 30 seconds to 1 minute.

Several changes of water for 30 seconds to 1 minute each were used for destaining the membranes. Stop the destaining as soon as the background got slight pink. The intensity of the bands on the membrane could be used for the rough quantifications of proteins on PVDF or nitrocellulose membranes [21]. The membrane was then blocked with 5% nonfat dry milk in TBST (50 mM Tris-HCl pH 7.5, 200 mM NaCl, 0.05% Tween-20) at room temperature for 30 minutes. It was washed briefly with TBST, and incubated with individual mouse serum in 1% milk in TBST for 1 hour at room temperature, or overnight at 4 °C. The mouse plasmas were obtained from participating mice after euthanization. Briefly, whole blood was collected and put into EDTA-treated tubes. Cells were removed by centrifugation for 15 minutes at 1,500x g. The resulting supernatant was designated plasma. After washing the membrane with TBST three times (10 minutes each), it was incubated with the secondary antibody at room temperature for 1 h. The goat anti-mouse IgG-HRP antibody was purchased from Santa Cruz Biotechnology (sc-2005). The membrane was then washed three times with TBST, treated with ECL detection reagents, and exposed to BlueBlot^{TM}HS film from Life Science Products (XR-0810-100).

2.3. Microbial DNA Extraction

To collect the fecal samples, mice were placed in an empty sterile cage for 5–10 min and freshly dropped fecal pellets were collected aseptically into sterile tubes. To obtain the cecum contents, mice were euthanized and sacrificed. Ceca were immediately collected and stored at -80°C until use. DNA was extracted from fecal samples using the Omega Mag-Bind® Soil DNA 96 Kit (Omega Bio-tek Inc., Norcross, GA) according to the manufacturer's protocol. Isolated DNA was stored at -20°C until used for bacterial community analysis. The bacterial community was evaluated using the V4

region of the 16S rDNA. Briefly, the V4 region of the 16S rDNA gene was amplified using barcoded universal primers and was multiplexed and sequenced using the MiSeq Illumina platform using 250bp paired end sequencing using the V2 500 cycle reagent kits. Library preparation PCR contained, 0.75 Units of Terra PCR Direct Polymerase Mix, 1X Terra PCR Direct Buffer, 0.4 uM indexed primers, and 10 – 25 ng of DNA. Cycling conditions included, initial denaturation of 98 °C for 2 min, followed by 25 cycles of 98°C for 10 s, 55°C for 30 s, and 68°C for 30 s; and a final extension of 68 °C for 4 min. The resulting PCR amplicons were normalized using the Charm Biotech Normalization Kit (Charm Biotech, San Diego, CA) following the manufacturer's protocol. Normalized libraries were pooled and were further purified using NucleoSpin® Gel and PCR Clean-up (Macherey-Nagal Inc, Bethlehem, PA). The resulting libraries were subjected to 250bp pair end sequencing using the Illumina MiSeq System (Illumina, San Diego, CA) using the V2 500 cycle sequencing kit as described by the manufacturer.

2.4. Data Processing pipeline

The DADA2 v1.10.1 pipeline was used to identify bacterial community changes as described previously [22]. In short, low-quality reads with a Q score of ≥25 were removed and the reads were trimmed to a consistent length of 200 bp. Error rates were estimated to distinguish rare variants from sequencing or base calling errors and contigs were assembled using the forward and reverse reads to generate contigs for the V4 region. Furthermore, quality filtering was performed to remove sequences with ambiguous bases, incorrect contig length, or assembly. Taxonomy was assigned using SILVA reference alignment database v132 and a phylogenetic tree was generated in MOTHUR (v.1.42.1). The resulting normalized (DeSeq2) ASV table was used for Principal

Coordinate Analysis (PCoA) using a weighted unifrac matrix within R by using the package ggplot2 (Wickham 2009). The weighted Unifrac distance matrix was used to perform multivariate analysis of variance (PERMANOVA) within the R package vegan.

2.5. Magnetic Resonance Imaging (MRI)

MRI was performed on a 7 Tesla small animal scanner (Bruker PharmaScan 70/16, Billerica, MA) operated using ParaVison 6.01. A Bruker made mouse head quadrature RF coil was used for signal transmitting and receiving. Mice were anesthetized by inhalation of 1-2% isoflurane in oxygen during scanning, and respiration and body temperature were monitored (Model 1025 Monitoring & Gating System, Small Animal Instruments, Inc., Stony Brook, NY). T_2-weighted coronal brain images were first obtained using Rapid Acquisition with Relaxation Enhancement (RARE) as an anatomical reference (TR/TE = 4200/48 ms, FOV = 20 x 20 mm^2, matrix size = 256 x 192, 21 slices, slice thickness = 0.5 mm, and averaging = 2). T_1-weighted and T_1 mapping scans were performed before and after intraperitoneal (i.p.) administration of gadolinium (MultiHance, Bracco Imaging) at 0.2 mM/kg. Modified driven equilibrium Fourier transform (MDEFT) was used for T1-weighted imaging with TR/TE/TI = 2600/2.2/950 ms, flip angle = 15^o, FOV = 20 x 20 mm^2, matrix size = 256 x 256, 15 slices and slice thickness = 0.5 mm. T_1 mapping data acquired using variable TR RARE (RAREVTR) with 6 TRs from 9 to 0.4 s. Other parameters included TE = 8 ms, FOV = 20 x 20 mm^2, matrix size = 96 x 128, 15 slices with slice thickness = 0.5 mm. T1 maps were calculated using an in-house developed fitting program written in IDL. T1 values on somatosensory cortex, hippocampus, striatum, thalamus and hypothalamus using region-of-interest (ROI) analysis.

2.6. Statistical analysis

Mann-Whitney U one-tailed test analyses were done with the use of Mann-Whitney U Test Calculator (https://www.socscistatistics.com/tests/mannwhitney/default2.aspx). General statistical analyses were performed by functions implemented in Microsoft Excel Program. Two group comparisons were done with Student's two-tailed unpaired t-test. The p values of < 0.05 were considered statistically significant and highly significant if $p < 0.01$ in all analyses.

3. Results

3.1. EBV-immortalized cells exacerbate EAE responses in mice During IM, EBV-infected B lymphocytes proliferate excessively and elicit strong immune responses, as they are viewed as foreign by the human immune system [9,23,24]. One of immune responses is the induction of heterophile antibodies. The well-established monospot test for IM diagnosis is based on the detections of heterophile antibodies [25]. There are several types of EBV-infected cell types and latency III latency cells are one of the predominant ones during IM [8,26]. Healthy EBV-carriers may occasionally have expansions of EBV-infected B lymphocytes and those cells are quickly removed by the EBV-specific immune cells [6,26-29]. The occasional expansions of EBV-infected cells are believed to be type III latency cells as EBV-specific CTLs are predominantly against type III latency antigens in EBV carriers[30]. If immune system had been suppressed, EBV-infected cells (type III latency) may quickly expand as in the case of post-transplant lymphoproliferative disorder [31,32]. We reasoned that xenografts of EBV-immortalized B lymphocytes (type III latency) into mice could partially mimic the

overproliferation of EBV-infected cells *in vivo* during mononucleosis and in a healthy EBV-carrier.

EBV-immortalized B lymphocytes from a SPMS patient (MS-LCL) were xenografted into C57BL/6 mice with intraperitoneal injections (i.p.). The age of mice was chosen at 4 weeks, which might be similar to human adolescent, a highly susceptible period for IM [33]. First, we found that C57BL/6 could tolerate 10^7 MS-LCL cells without any apparent effects for a certain period of times. The 10^7 MS-LCL cells were injected into mice every 10-14 days until euthanization (i.p., 5-7 times). No EAE symptoms appeared in mice given MS-LCL cells alone (data not shown). Therefore, EBV-immortalized cells *per se* did not induce EAE in C57BL/6 mice under our experimental conditions.

To test whether EBV is a priming factor for MS [34], we xenografted MS-LCL into C57BL/6 mice twice, and then the mice were immunized with MOG peptide using a standard EAE protocol (Figure 1A) [19]. The dosages for MOG peptide were screened first and the amounts for minimum EAE inductions were chosen (data not shown). As shown in Figure 1B, the MS-LCL inoculation enhanced EAE clinical scores. After EAE remission, EBV-infected cells or PBS were administrated into the mice again without MOG peptide. In this case MS-LCL alone stimulated an EAE relapse (Figure 1B; data after Day 29). Therefore, the xenografts of EBV-infected cells could enhance the EAE development in a statistically significant manner.

To verify the enhancement was not a dosage issue, we used a different mouse line that is known to be more sensitive to EAE. APP is a protein involved in the pathogenesis of brain diseases [35]. APP-null mice are more sensitive for EAE inductions

[18]. APP-null mice were concurrently used for the same experiments. No statistical significant enhancements were observed in APP-null mice administered MS-LCL with the same protocol (Figure 1C). The phenotypes of APP-null mice were as previously reported: earlier EAE onset, higher clinical scores (compare PBS-treatments between APP-null and C57BL/6), and without remission (Figure 1C) [18]. The data in APP-null mice confirmed that the dosages for EAE inductions were properly selected in the C57BL/6 mice.

Because we have used MS patient-derived EBV-immortalized B lymphocytes, it is therefore possible that the MS-specific factor(s) derived from these B cells is involved. This possibility is eliminated as EBV-immortalized cells from healthy non-MS individuals also have similar effects (data not shown). All those data suggest that mimicking IM in mice may potentiate EAE development.

3.2. Challenge with EBV-immortalized cells after EAE remission induces a relapse. It is reasonable to assume that the occasional overproliferation of EBV-positive cells is present in remission stages of MS patients. As EBV-immortalized cells might be involved in exacerbating EAE (Figure 1B), we addressed whether there was an enhancement in the relapse without prior treatment of EBV-immortalized cells. C57BL/6 mice were primed with MS-LCL or PBS prior to initiation of EAE protocol. After EAE remission, both groups were challenged with the same MS-LCL cells. As seen before, EBV-immortalized MS-LCL caused EAE relapse without further injection of MOG peptide. It was apparent that the additional challenge induced a relapse (secondary EAE) predominantly in EAE mice primed with MS-LCL (Figure 2A). Because of the sample size, we did additional experiments to address whether prior exposure to MS-LCL was necessary for a relapse. As shown in Figure 2B, the prior

MS-LCL treatment was required for the relapse without further MOG treatment. Furthermore, we observed that clinical peak scores of the relapses basically aligned with the previous clinical scores of the mice induced by MOG peptides.

To test if the mice had immune responses to EBV-immortalized cells, we collected plasmas from several MS-LCL xenografted or PBS-treated mice, and used them for Western Blot analysis with identical conditions. The plasmas reacted with MS-LCL lysates pretty strongly (data not shown), which indicate that MS-LCL induced immune responses against itself. Next whether MS-LCL xenografted mice had a specific antibody to EBV latent proteins was examined. Sav I and SavIII are isogenic lines with different EBV-latencies: SavI has only one EBV protein expression (type I latency), while SavIII has eight or more viral protein expressed (type III latency)[4,36,37]. SavIII and MS-LCL are not the same lines but they have the same EBV latency type. As shown in Figure 2C, a MS-LCL xenografted mouse had strong antibody responses to EBV-infected human B lymphocytes. Unfortunately, no convincing evidence that specific antibodies to EBV latent antigens generated as the EBV-negative ones also react with the plasmas. Moreover, different plasmas provided different patterns of reactions (data not shown). However, the data in Figure 2C clearly showed that xenografted mice had immune response to human B lymphocytes.

3.3. EBV-immortalized cells elicit changes in gut microbiome associated with EAE progression Recent evidence suggests alterations in the gut microbiome of MS patients may be a contributor towards the promotion of inflammatory cytokines and overall inflammation [38]. Moreover, changes in microbiota composition may result in imbalances in metabolites produced and nutrients available leading to diseases. As

such, modulation of the gut microbiome can be viewed as a potential novel therapeutic avenue [38-40].

To evaluate the possible associations between the gut microbiota and EAE progression, we performed longitudinal evaluation of the gut microbiota composition as described in Figure 1B and Supplemental Table 1. Basically the feces were collected on the Day 16, 28, 36, and 50. Ceca were collected on the Day 51 after euthanization. The V4 region of the 16S rDNA gene was amplified using barcoded universal primers and was multiplexed as previously described[41]. Resulting amplicons were sequenced using a MiSeq Illumina platform with 250-bp paired end sequencing[41]. The eubacterial community of the fecal microbiota was analyzed using Amplicon Sequence Variant (ASV) using the Dada2 pipeline [42]. Alpha diversity metrics between the two treatment groups displayed significant differences in bacterial diversity across time periods (p= 0.026 – 0.001). Additionally, beta-diversity analysis using weighted-UniFrac [43] demonstrated significant differences in microbial community compositions between PBS and MS-LCL treated mice as a whole (p<0.009) and in a longitudinal manner (p<0.001) (Fig 3A). The changes in microbial community were associated with time of sampling, including higher abundance of phylum *Verrucomicrobia* during the initial sampling period followed by a decrease in abundance of this taxa over time. Additionally, the phyla *Firmicutes* and *Bacteriodetes* fluctuated over time (Fig 3B). Further analysis of bacterial taxa following the first MS-LCL injection demonstrated an increase of *Ruminococococceae*, and *Muribaculaceae* families in comparison to PBS treated mice. However, different trends were observed with the third MS-LCL treatment (D29): an increase of families of *Lachinospiraceae* and *Ruminococaceae*, and a decrease in *Akkermansiaceae* family (Fig 3C). Of note that *Akkermansiaceae* has

apparent anti-inflammatory functions [44-46]. Four female mice (F16-F19, Supplemental Table 1) from the same litter were maintained in the same cage. They had received the same MS-LCL treatment but presented with different clinical scores that could be classified into two groups (Supplemental Figure 1). The differential analysis of bacterial taxa between the two phenotypes in this cage displayed differences in taxa abundance of *Lachinospireceae* (Fig 3D). In summary, bacterial community composition significantly changed with MS-LCL xenografts.

3.4. Xenografts of EBV-immortalized cells enhance the integrity of blood brain barriers (BBB) in mice The BBB is a highly selective permeability barrier that separates circulating blood from the brain's extracellular fluid in the CNS. Because of tight junctions, BBB may prevent the entry of potential neurotoxins. It is generally accepted that some cells/factors must cross the BBB and enter the CNS for MS pathogenesis [47].

Because EBV-infected cells were capable of enhancing EAE scores (Figures 1 and 2), whether those cells could affect BBB permeability before the onset of EAE was examined. Mice were xenografted with MS-LCL or PBS, followed by EAE induction. Before the onset of EAE (Days 8 and 9), the BBB integrities of the mice were assessed with gadolinium (Gd)-enhanced magnetic resonance imaging (MRI). The reason to choose MRI over other methods is that MRI can monitor the BBB integrity in a non-invasive manner. Several areas in the mouse brains were examined systemically, including striatum (STR), hippocampus (HP), thalamus (TH), hypothalamus (HY) and cerebral cortex (CTX). T1-weighted images were taken prior to and after Gd injection and compared. The post-contrast signal intensity in the PBS-control mice might be higher than the MS-LCL-injected mice, suggesting that higher Gd deposition in the

PBS control mice (Figure 4A). Furthermore, T1 values on various areas were measured using region-of-interest (ROI) analyses. The T1 shortening in a region suggests the Gd entry of brain parenchyma and a strong indicator of comprised BBB integrity [48]. Gd-induced T1-shortening was found in all animals by comparing pre- and post-Gd T1 values, but was only statistically significant on TH and STR in PBS control mice (Figure 4B). The results suggested that the MOG/CFA injection *per se* could enhance BBB disruptions in TH and STR areas. The comparisons of PBS- and MS-LCL-treated groups showed that post-Gd T1 values in PBS-treated mice are significantly lower than in MS-LCL-treated mice on HY and TH (Figure 4B). The results suggested EBV-immortalized cells induced tighter BBB integrities in the HY and TH regions under the current experimental conditions. This result underscores that extent and regional specificity of BBB damage may differ among individual EAE models with different methods for detections.

4. Discussion

4.1. Potential novel rodent model for human RRMS Approximately 85-90% of individuals with MS are initially diagnosed as RRMS. A relapsing-remitting EAE (RR-EAE) model, representing a course of exacerbations and remissions as occurs in human MS, will be extremely useful for both basic research and translational studies. Pathophysiological RR-EAE can be induced by passive transfer of the proteolipid protein (PLP) reactive cell lines that involve the immunization of donor mice with PLP peptides. Additionally, MOG, myelin basic protein (MBP) peptides and MBP reactive T cell clones are also used to induce RR-EAE [16,49-51].

By mimicking behavior of EBV-infected B-lymphocytes in IM *in vivo*, we have shown that xenografts of EBV-immortalized B lymphocytes could induce a second EAE response (relapse) (Figures 1, 2). The relapse can be reproducibly generated from remitting mice. The unique feature of the system is that severity of the relapse can be predicted based on previous clinical scores (Figure 2B). In addition, onset time of the relapses can also be predicted. This model might be an additional beneficial one for RR-EAE and furthermore RRMS in humans. However, more biochemical and pathogenic studies are warranted to verify the current one as a human RRMS model.

4.2. EBV-mediated B cell proliferation in MS development There are several possible explanations for the EAE exacerbation by EBV-infected B cells (Figures 1,2). One of them is that the EBV-induced proliferation of B lymphocytes or elevated presence of B lymphocytes, is a possible factor in MS development. In a healthy individual, hyperproliferation of B lymphocytes may be a stress factor for the immune system, which is likely to initiate a counteracting response. The process to reduce the excessive B lymphocytes may be a trigger for exacerbation of MS. The linkage between EBV and MS may be related to the fact that EBV induces overproliferation of B cells during primary IM and small but frequent B cell proliferation during asymptomatic phase. Of note, MS is associated with deficiencies in EBV-specific cytotoxic T lymphocyte (CTL) and uncontrolled lytic replication [13,52,53]. CTL deficiency would allow the expansion of EBV-infected cells as in immunodeficient situations, and higher lytic replication would lead to more EBV virions that promote B cells proliferation after primary infection [4]. Therefore, both associations may result in a hyperproliferation of EBV-infected B cells *in vivo*. It is noteworthy that clinically

reductions in B lymphocytes is viewed as a good treatment for MS [54]. It is therefore tempting to speculate that EBV-mediated B cell proliferation *in vivo* is a factor in the development or exacerbation of MS.

Our hypothesis about EBV's role in MS is different from current hypothesized ones [13,52], in that it puts the overproliferation of B lymphocytes, rather than EBV *per se*, as a potential risk factor for MS development. Majority of literature support the notion that MS is associated with IM. Primary EBV infection may account for 90% of the IM cases, and a growing number of pathogens, such as cytomegalovirus, have been reported to cause mononucleosis-like illnesses [24,55,56]. The literature related IM and MS might need re-evaluated with careful etiology of IM examinations. The bacterial infection might play an important role in precipitating relapse in MS [57,58]. Of note bacterial infections may cause B cell proliferation [59]. Therefore, our hypothesis about EBV, B lymphocytes, and MS may extend to other infectious agents or beyond.

It is surprising that the challenge of EBV-infected cells actually tightens BBB before the onset of EAE (Figure 4). Because preventing BBB untightening is associated with reduced EAE in at least SJL mice [60], our study suggests that extent and regional specificity of BBB damage differ between individual EAE models and/or at different stages.

Xenografts of EBV-immortalized cells were clearly associated with the modulation of the gut microbiome components (Figure 3A). It is possible that gut microbiome changes may result in changes in microbial metabolic end products in the gut that are associated with EAE[61-64]. From this limited study, *Akkermansiaceae* is apparently decreased after xenografts, and the supplementation of the bacteria, which is

apparently safe and effective for other disease [65], might be good for inhibition of EAE/MS.

In summary, our data collectively suggest that overproliferation of EBV-infected B lymphocytes may be a risk factor for the exacerbation of MS, whereby changes are associated with the gut microbiome and BBB. Furthermore, the data herein suggest that xenografts of EBV-immortalized cells might be a useful adjunct for RR-EAE model with a predictable severity and timing in C57BL/6 mice.

Acknowledgement

We thank Multiple Sclerosis Genetic Susceptibility Project at UCSF for providing EBV-immortalized MS patient's B lymphocytes, Dr. Jeff Sample for Sav I and III lines, and Dr. Jay Reddy for reviewing the manuscript. This work was made possible by grants from the Laymen Award, Revision Award from UNL, National Institute of General Medical Sciences, 1U54GM115458, which funds the Great Plains IDeA-CTR Network (LZ), Nebraska Research Initiative (YL), and USDA National Institute of Food and Agriculture (2018-67015-27496, 2018-68003-27545, and 1000579) (SCF). PP was a Fogarty fellow supported in part by the NIH Fogarty International Center grant D43TW010354.

Author Contribution L.Z. conceived the experiment, together with P.P., A.B., T.P., S.F. carried it out; Y.L. was responsible for MRI works and analyses. LZ wrote the paper.

Conflict of Interest Statement: The authors certify that they have NO affiliations with or involvement in any organization or entity with any financial interest.

References

1. Goldenberg MM. Multiple sclerosis review. *P T.* 2012;37(3):175-184.

2. Gold R, Wolinsky JS, Amato MP, Comi G. Evolving expectations around early management of multiple sclerosis. *Ther Adv Neurol Disord.* 2010;3(6):351-367.

3. Milo R, Miller A. Revised diagnostic criteria of multiple sclerosis. *Autoimmun Rev.* 2014;13(4-5):518-524.

4. Pagano JS. Epstein-Barr virus: the first human tumor virus and its role in cancer. *Proc Assoc Am Physicians.* 1999;111:573-580.

5. Cohen JI. Epstein-barr virus vaccines. *Clin Transl Immunology.* 2015;4(1):e32.

6. Kieff E. Epstein-Barr virus and its replication. In: Fields BN, Knipe DM, Howley PM, eds. *Virology, 3rd Edition.* Philadelphia, PA: Lippinscott-Raven Publishers; 1996:2343-2396.

7. Abbott RJ, Pachnio A, Pedroza-Pacheco I, et al. Asymptomatic Primary Infection with Epstein-Barr Virus: Observations on Young Adult Cases. *J Virol.* 2017;91(21).

8. Kurth J, Spieker T, Wustrow J, et al. EBV-infected B cells in infectious mononucleosis: viral strategies for spreading in the B cell compartment and establishing latency. *Immunity.* 2000;13(4):485-495.

9. Niedobitek G, Agathanggelou A, Herbst H, Whitehead L, Wright DH, Young LS. Epstein-Barr virus (EBV) infection in infectious mononucleosis: virus latency, replication and phenotype of EBV-infected cells. *J Pathol.* 1997;182(2):151-159.

10. Nielsen TR, Rostgaard K, Nielsen NM, et al. Multiple sclerosis after infectious mononucleosis. *Arch Neurol.* 2007;64(1):72-75.

11. Goldacre MJ, Wotton CJ, Seagroatt V, Yeates D. Multiple sclerosis after infectious mononucleosis: record linkage study. *J Epidemiol Community Health.* 2004;58(12):1032-1035.

12. Thacker EL, Mirzaei F, Ascherio A. Infectious mononucleosis and risk for multiple sclerosis: a meta-analysis. *Ann Neurol.* 2006;59(3):499-503.

13. Pender MP, Burrows SR. Epstein-Barr virus and multiple sclerosis: potential opportunities for immunotherapy. *Clin Transl Immunology.* 2014;3(10):e27.

14. Pakpoor J, Giovannoni G, Ramagopalan SV. Epstein-Barr virus and multiple sclerosis: association or causation? *Expert Rev Neurother.* 2013;13(3):287-297.

15. Tselis A. Epstein-Barr virus cause of multiple sclerosis. *Curr Opin Rheumatol.* 2012;24(4):424-428.

16. Robinson AP, Harp CT, Noronha A, Miller SD. The experimental autoimmune encephalomyelitis (EAE) model of MS: utility for understanding disease pathophysiology and treatment. *Handb Clin Neurol.* 2014;122:173-189.

17. Constantinescu CS, Farooqi N, O'Brien K, Gran B. Experimental autoimmune encephalomyelitis (EAE) as a model for multiple sclerosis (MS). *Br J Pharmacol.* 2011;164(4):1079-1106.

18. Grant JL, Ghosn EE, Axtell RC, et al. Reversal of paralysis and reduced inflammation from peripheral administration of beta-amyloid in TH1 and TH17 versions of experimental autoimmune encephalomyelitis. *Sci Transl Med.* 2012;4(145):145ra105.

19. Bittner S, Afzali AM, Wiendl H, Meuth SG. Myelin oligodendrocyte glycoprotein (MOG35-55) induced experimental autoimmune encephalomyelitis (EAE) in C57BL/6 mice. *J Vis Exp.* 2014(86).

20. Stromnes IM, Goverman JM. Passive induction of experimental allergic encephalomyelitis. *Nature Protocols.* 2006;1(4):1952-1960.

21. Salinovich O, Montelaro RC. Reversible staining and peptide mapping of proteins transferred to nitrocellulose after separation by sodium dodecylsulfate-polyacrylamide gel electrophoresis. *Anal Biochem.* 1986;156(2):341-347.

22. Callahan BJ, McMurdie PJ, Rosen MJ, Han AW, Johnson AJ, Holmes SP. DADA2: High-resolution sample inference from Illumina amplicon data. *Nat Methods.* 2016;13(7):581-583.

23. Womack J, Jimenez M. Common questions about infectious mononucleosis. *Am Fam Physician.* 2015;91(6):372-376.

24. Balfour HH, Jr., Dunmire SK, Hogquist KA. Infectious mononucleosis. *Clin Transl Immunology.* 2015;4(2):e33.

25. Marshall-Andon T, Heinz P. How to use... the Monospot and other heterophile antibody tests. *Arch Dis Child Educ Pract Ed.* 2017;102(4):188-193.

26. Hadinoto V, Shapiro M, Greenough TC, Sullivan JL, Luzuriaga K, Thorley-Lawson DA. On the dynamics of acute EBV infection and the pathogenesis of infectious mononucleosis. *Blood.* 2008;111(3):1420-1427.

27. Silins SL, Cross SM, Krauer KG, Moss DJ, Schmidt CW, Misko IS. A functional link for major TCR expansions in healthy adults caused by persistent Epstein-Barr virus infection. *J Clin Invest.* 1998;102(8):1551-1558.

28. Rickinson AB, Kieff E. Epstein-Barr Virus. In: Fields BN, Knipe DM, Howley PM, eds. *Virology, 3rd Edition.* Philadelphia, PA: Lippinscott-Raven Publishers; 1996:2397-2446.

29. Leen A, Meij P, Redchenko I, et al. Differential immunogenicity of Epstein-Barr virus latent-cycle proteins for human CD4(+) T-helper 1 responses. *J Virol.* 2001;75(18):8649-8659.

30. Rickinson AB, Lee SP, Steven NM. Cytotoxic T lymphocyte responses to Epstein-Barr virus. *Curr Opin Immunol.* 1996;8(4):492-497.

31. Green M, Michaels MG. Epstein-Barr virus infection and posttransplant lymphoproliferative disorder. *Am J Transplant.* 2013;13 Suppl 3:41-54; quiz 54.

32. Gottschalk S, Rooney CM, Heslop HE. Post-transplant lymphoproliferative disorders. *Annu Rev Med.* 2005;56:29-44.

33. Dutta S, Sengupta P. Men and mice: Relating their ages. *Life Sci.* 2016;152:244-248.

34. Kakalacheva K, Regenass S, Wiesmayr S, et al. Infectious Mononucleosis Triggers Generation of IgG Auto-Antibodies against Native Myelin Oligodendrocyte Glycoprotein. *Viruses.* 2016;8(2).

35. O'Brien RJ, Wong PC. Amyloid precursor protein processing and Alzheimer's disease. *Annu Rev Neurosci.* 2011;34:185-204.

36. Zhang L, Pagano JS. IRF-7, a new interferon regulatory factor associated with Epstein-Barr virus latency. *Mol Cell Biol.* 1997;17:5748-5757.

37. Zhang L, Pagano JS. Interferon Regulatory Factor 2 Represses the Epstein-Barr Virus BamH I Q Latency Promoter In Type III Latency. *Mol Cell Biol.* 1999;19:3216-3223.

38. Kirby TO, Ochoa-Reparaz J. The Gut Microbiome in Multiple Sclerosis: A Potential Therapeutic Avenue. *Med Sci (Basel).* 2018;6(3).

39. McCarville JL, Caminero A, Verdu EF. Novel perspectives on therapeutic modulation of the gut microbiota. *Therap Adv Gastroenterol.* 2016;9(4):580-593.

40. Marchesi JR, Adams DH, Fava F, et al. The gut microbiota and host health: a new clinical frontier. *Gut.* 2016;65(2):330-339.

41. Kozich JJ, Westcott SL, Baxter NT, Highlander SK, Schloss PD. Development of a dual-index sequencing strategy and curation pipeline for analyzing amplicon sequence data on the MiSeq Illumina sequencing platform. *Appl Environ Microbiol.* 2013;79(17):5112-5120.

42. Callahan B, Proctor D, Relman D, Fukuyama J, Holmes S. REPRODUCIBLE RESEARCH WORKFLOW IN R FOR THE ANALYSIS OF PERSONALIZED HUMAN MICROBIOME DATA. *Pac Symp Biocomput.* 2016;21:183-194.

43. Lozupone CA, Hamady M, Kelley ST, Knight R. Quantitative and qualitative beta diversity measures lead to different insights into factors that structure microbial communities. *Appl Environ Microbiol.* 2007;73(5):1576-1585.

44. Zhai R, Xue X, Zhang L, Yang X, Zhao L, Zhang C. Strain-Specific Anti-inflammatory Properties of Two Akkermansia muciniphila Strains on Chronic Colitis in Mice. *Front Cell Infect Microbiol.* 2019;9:239.

45. Derrien M, Belzer C, de Vos WM. Akkermansia muciniphila and its role in regulating host functions. *Microb Pathog.* 2017;106:171-181.

46. Naito Y, Uchiyama K, Takagi T. A next-generation beneficial microbe: Akkermansia muciniphila. *J Clin Biochem Nutr.* 2018;63(1):33-35.

47. Minagar A, Alexander JS. Blood-brain barrier disruption in multiple sclerosis. *Multiple sclerosis.* 2003;9(6):540-549.

48. Ku MC, Waiczies S, Niendorf T, Pohlmann A. Assessment of Blood Brain Barrier Leakage with Gadolinium-Enhanced MRI. *Methods Mol Biol.* 2018;1718:395-408.

49. Zamvil S, Nelson P, Trotter J, et al. T-cell clones specific for myelin basic protein induce chronic relapsing paralysis and demyelination. *Nature.* 1985;317(6035):355-358.

50. Tuohy VK, Lu Z, Sobel RA, Laursen RA, Lees MB. Identification of an encephalitogenic determinant of myelin proteolipid protein for SJL mice. *J Immunol.* 1989;142(5):1523-1527.

51. Berard JL, Wolak K, Fournier S, David S. Characterization of relapsing-remitting and chronic forms of experimental autoimmune encephalomyelitis in C57BL/6 mice. *Glia.* 2010;58(4):434-445.

52. Pender MP. The essential role of Epstein-Barr virus in the pathogenesis of multiple sclerosis. *Neuroscientist.* 2011;17(4):351-367.

53. Angelini DF, Serafini B, Piras E, et al. Increased CD8+ T cell response to Epstein-Barr virus lytic antigens in the active phase of multiple sclerosis. *PLoS Pathog.* 2013;9(4):e1003220.

54. Baker D, Marta M, Pryce G, Giovannoni G, Schmierer K. Memory B Cells are Major Targets for Effective Immunotherapy in Relapsing Multiple Sclerosis. *EBioMedicine.* 2017;16:41-50.

55. Hurt C, Tammaro D. Diagnostic evaluation of mononucleosis-like illnesses. *Am J Med.* 2007;120(10):911 e911-918.

56. Taylor GH. Cytomegalovirus. *Am Fam Physician.* 2003;67(3):519-524.

57. Rapp NS, Gilroy J, Lerner AM. Role of bacterial infection in exacerbation of multiple sclerosis. *Am J Phys Med Rehabil.* 1995;74(6):415-418.

58. Metz LM, McGuinness SD, Harris C. Urinary tract infections may trigger relapse in multiple sclerosis. *Axone.* 1998;19(4):67-70.

59. Nothelfer K, Sansonetti PJ, Phalipon A. Pathogen manipulation of B cells: the best defence is a good offence. *Nat Rev Microbiol.* 2015;13(3):173-184.

60. Badawi AH, Kiptoo P, Wang WT, et al. Suppression of EAE and prevention of blood-brain barrier breakdown after vaccination with novel bifunctional peptide inhibitor. *Neuropharmacology.* 2012;62(4):1874-1881.

61. Lee YK, Menezes JS, Umesaki Y, Mazmanian SK. Proinflammatory T-cell responses to gut microbiota promote experimental autoimmune encephalomyelitis. *Proc Natl Acad Sci U S A.* 2011;108 Suppl 1:4615-4622.

62. Gandy KAO, Zhang J, Nagarkatti P, Nagarkatti M. The role of gut microbiota in shaping the relapse-remitting and chronic-progressive forms of multiple sclerosis in mouse models. *Sci Rep.* 2019;9(1):6923.

63. Berer K, Gerdes LA, Cekanaviciute E, et al. Gut microbiota from multiple sclerosis patients enables spontaneous autoimmune encephalomyelitis in mice. *Proc Natl Acad Sci U S A.* 2017;114(40):10719-10724.

64. Berer K, Mues M, Koutrolos M, et al. Commensal microbiota and myelin autoantigen cooperate to trigger autoimmune demyelination. *Nature.* 2011;479(7374):538-541.

65. Depommier C, Everard A, Druart C, et al. Supplementation with Akkermansia muciniphila in overweight and obese human volunteers: a proof-of-concept exploratory study. *Nat Med.* 2019;25(7):1096-1103.

Figures

Figure 1: Exacerbation of EAE in mice xenografted with EBV-immortalized cells. A, Mice are injected twice with EBV-immortalized cells (i.p.), then MOG immunization, and followed by another injection of EBV-immortalized cells when EAE score is low. Drawing is not on scale. **B,** the 4-week old C57BL/6 mice were first injected (i.p) with 10^7 EBV-immortalized SPMS-patient's B lymphocytes (MS-LCL) (dashed lines; two litters, 3 males, 4 females) or PBS (solid lines; two litters, 3 males, 3 females) twice at Day -31 and Day -22 respectively. EAE induction was following standard protocol with MOG peptide. Mean clinical scores and standard error of the mean (SEM) are shown. After the apparent remission of EAE (Day 29, indicated by an arrow), third injection (i.p) of MS-LCL (dashed line) or PBS (solid line) respectively was carried out. Mouse feces were collected at D16, D28, D36, and D50. At the D51, mice were euthanized and ceca were collected for microbiome analyses. At the end of the study, survival rates for all groups were 100%. Total 6 out 7 mice with MS-LCL injections, while 2 out 6 PBS-injected, developed EAE. The detailed information about mice and treatments are described in the Supplemental Table 1. Mann-Whitney U one-tailed analysis. *, $p \leq 0.05$; **, $p \leq 0.01$. **C,** APP-null mice (7-week old) were immunized with MS-LCL (dashed lines with blue dots; three litters: 3 males, 4 females) or PBS (solid lines with orange dots; three litters: 2 males, 3 females). All cells and reagents used were the same, and treatments were done simultaneously as in Panel B. At Day 29, third injection of MS-LCL or PBS respectively was carried out. At the end of the study, total 6 out 7 mice with MS-LCL injections, while 5 out 5 mice with PBS-injected, developed EAE. A higher rate of mortality was seen in APP-null mice with MS-LCL (3 out 7) compared with PBS (death 0 out 5, however one euthanized after reaching EAE score 4). No statistical significant differences were noticed between the two groups.

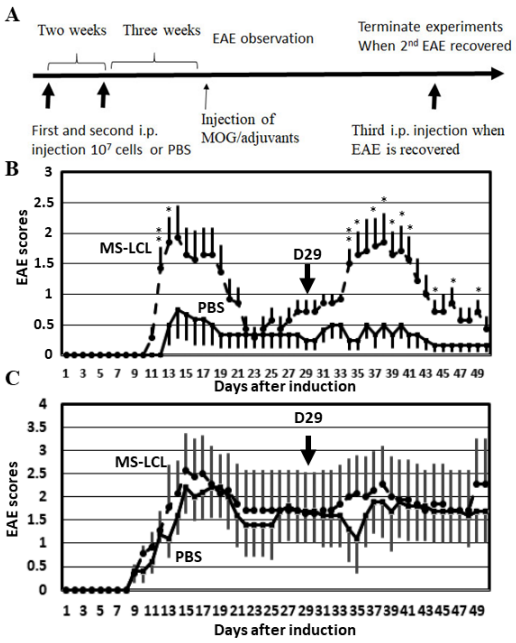

Figure 2: EBV-immortalized cells initiate second EAE response after remission. A, C57BL/6 mice were first immunized with MS-LCL as in Figure 1A (dashed lines; one litter: 2 males, 2 females) or PBS (solid lines; one litter: 1 male, 2 females) twice. MOG-CFA and others were injected as described in the Methods. The severity of EAE was scored on daily basis. After the apparent remission of EAE, all mice were injected (i.p.) with the same MS-LCL at Day 27, indicated by an arrow. At the end of the study, survival rates were 100%. Total 4 out 4 mice with MS-LCL injections, while 2 out 3 PBS-injected, developed EAE. Mean EAE clinical scores and standard error of the mean (SEM) were shown. Student t tests were performed by the use of Microsoft Excel. *, $p \leq 0.05$; **, $p \leq 0.01$. **B**, C57BL/6 mice were immunized with MS-LCL (two litters: 4 males, 4 females) or PBS (two litters: 3 males, 3 females) and followed by MOG-CFA injection as in Panel A. At Day 8 and 9, mice were examined by a MRI machine. All mice were injected (i.p.) with MS-LCL at remission stage. At the end of the study, survival rates were 100%. Total 7 out 8 mice with MS-LCL injections (average maximum score: 1.92), while 5 out 6 PBS-injected (average maximum score: 1.12), developed EAE. The first peak clinical scores were used as a base for calculation of the secondary induction efficiency (percentage). Mean secondary induction percentages and standard error of the mean (SEM) were shown. Mann-Whitney U one-tailed analysis. *, $p \leq 0.05$; **C,** the plasmas from MS-LCL injected and PBS control mice (after three injections) were used for Western Blot analysis as primary antibodies with identical conditions. SavIII and MS-LCL are not the same lines but they have the same type III EBV latency. Each lane contained approximately the same amounts of proteins as determined by ponceau S staining (data not shown), and the protein markers were used to facilitate the cutting the membrane into pieces. Each piece was used for

incubation with one plasma at the same dilutions. They were pieced together for final exposure. Molecular weight makers (in kDa) are shown.

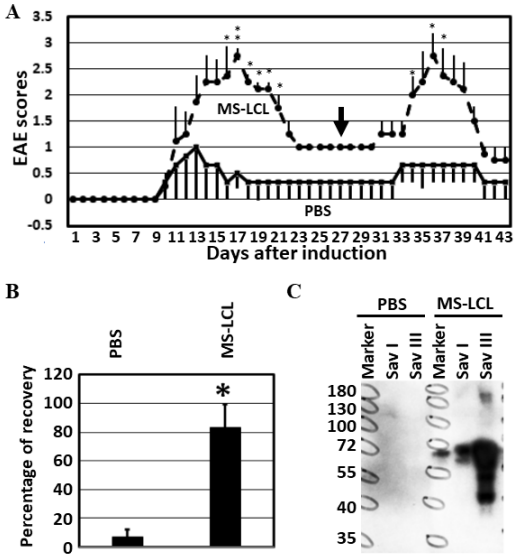

Figure 3. Gut microbiota community changes in response to Xenografts of EBV-immortalized cells. Fecal samples were collected as described in Supplemental Table 1 and the microbial community was analyzed using 16S rDNA sequencing of the V4 region using the MiSeq Illumina platform. The eubacterial community of the fecal microbiota was analyzed using Amplicon Sequence Variant (ASV) using the Dada2 pipeline. **A,** Beta-diversity plot showing microbial community differences by treatment and time. Colors represent individual mouse identities, shape represents time and size of shape represents treatment. The individual identities and treatments are listed in the Supplemental Table 1. **B,** Heatmap showing the relative abundances of the most abundant phyla in mice sampled five times. Phylum assignments are shown with different colors. The F13-F25 represents the identities of individual mice. The number followed represents the dates of the collections. 1=D16, 2=D28, 3=D36, 4=D50, and 5=D51 (Figure 1B). Treatments are also indicated at the bottom. **C,** Heatmap of differential ASVs identified in each treatment group at the time when differences of EAE scores were observed. Collection dates are shown on the top, and the treatments are shown at the bottom. Mouse numbers are not shown but can be identified from the position: from left to right: F13->F19 in MS-LCL treatments, and F20->F25 in PBS controls as in Panel B. **D**, Differential ASVs are identified in the cage where the four mice from the same litter, same sex (F), and same treatment (MS-LCL). The identities of the mice are as shown. The F16 and F18 mice had higher EAE clinical scores (Supplemental Figure 1). The collection dates are shown on the top.

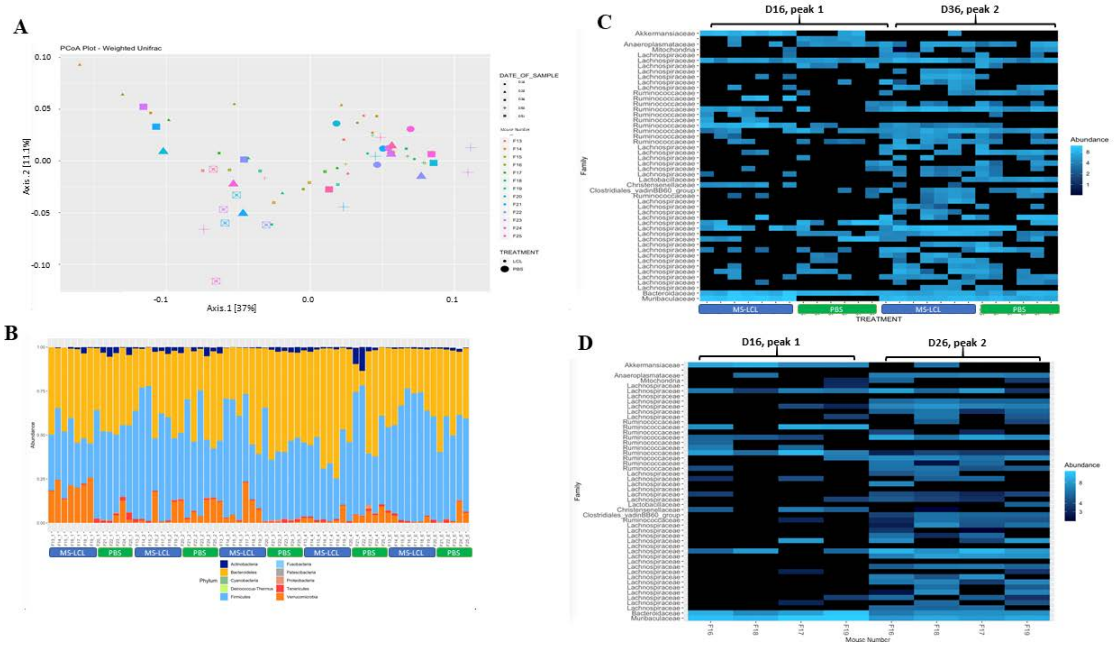

Figure 4: **EBV-immortalized cells may tighten the BBB in certain areas of mouse brains**. **A,** Mice were treated as described in details in Figure 2B. At Day 8 and 9 after MOG-CFA inductions, mice were examined by MRI. No mice had shown any EAE signs at the time of examinations. Typical pre- and post-contrast T1-weighted images of PBS- and LCL-treated mice are shown. Top row: a PBS-treated mouse, bottom row: a MS-LCL-treated mouse. Striatum (STR), hippocampus (HP), thalamus (TH), hypothalamus (HY) and cerebral cortex (CTX) arears are indicated. Scale bar: 2 mm. **B,** MRI obtained T1 values on HY, TH, STR, SM, CTX, and HP measured using ROI analyses. The T1 shortening on all regions suggests gadolinium entry of brain parenchyma. The T1 shortening effect is significant on TH and STR in PBS-treated mice. T1 values on HY and TH in PBS-treated mice are significantly lower than in LCL-treated mice. Mann-Whitney U one-tailed analysis. *, $p \leq 0.05$;